Solid-State Electronics Pergamon Press 1961. Vol. 2, pp. 165–189. Printed in Great Britain

MECHANISMS OF SPACE-CHARGE-LIMITED CURRENT IN SOLIDS

G. T. WRIGHT

Electrical Engineering Department, University of Birmingham

(*Received* 18 *August* 1960; *in revised form* 17 *October* 1960)

Abstract—The mechanisms of space-charge-limited (SCL) current in solids are discussed. The practical case is taken of a wide band-gap, high-resistivity material containing empty shallow trapping states but in which empty deep trapping states are eliminated by the mechanism of defect compensation described by LONGINI and GREEN (1956). One-dimensional and one-carrier (electron) current through a plane parallel crystal is considered for the case when one contact is ohmic and one contact is blocking.

At small forward voltage, current occurs by the predominant mechanism of carrier diffusion and increases approximately as the exponential of applied voltage; in this range, current is very sensitive to temperature changes. At large forward voltage, current occurs by the predominant mechanism of carrier drift and, after a voltage threshold due to the work-function difference between anode and cathode metals, increases very nearly as the square of applied voltage; this result confirms the simplified analysis of MOTT and GURNEY (1940) and is the solid-state analogue of the three-halves power law for space-charge-limited current in vacuum. In this range current varies as the inverse cube of crystal thickness and is relatively insensitive to temperature changes. Between these two current ranges a smooth transition occurs from a diffusion to a drift mechanism of current and a "virtual cathode" is established in the crystal; there is no evidence for the existence of a negative-resistance region during the transition as predicted by SKINNER (1955). Simple and accurate analytic expressions are derived describing forward current–voltage characteristics in the exponential and square-law ranges; they show that, depending mainly on crystal thicknesses, high forward conductance or high forward resistance can be achieved. With a strongly blocking anode, reverse current is always very small and very high rectification ratios can be achieved.

For current in the square-law range the Fermi-level is nearly constant through the crystal, except near the cathode and anode contacts. This justifies the distinction made by ROSE (1955) between shallow traps, which lie above the Fermi-level and do not affect the form of the current–voltage characteristics, and deep traps, which lie below the Fermi-level and profoundly modify the current–voltage characteristics.

The discussion is illustrated with numerical results calculated on the basis of an electron mobility of 1000 cm^2/V-sec which is intermediate between the value of 200 cm^2/V-sec for cadmium sulphide and 9300 cm^2/V-sec for gallium arsenide. In conclusion, some possible applications are considered for space-charge-limited current in fundamental solid-state research.

Résumé—Les mécanismes du courant à charge d'espace limitée dans les solides sont décrits. Le cas pratique est considéré pour un matérial, ayant une haute résistivité et une large zone interdite, contenant des états de trappe vides et bas, mais dans lequel les états de trappe vides et profonds sont éliminés par le mécanisme de compensation de défaut décrit par LONGINI et GREEN (1956). Le courant d'une dimension et d'un porteur (électron) est décrit pour le cas où un contact est ohmique et un contact est de verrouillage.

A une petite tension de sens avant, le courant est determiné par le mécanisme prédominant de diffusion de porteurs et augmente approximativement en fonction exponentielle de la tension appliquée; dans cette gamme, le courant est très sensible aux variations de la température. A une haute tension de sens avant, le courant est determiné par le mécanisme prédominant d'apport de porteurs et, après une certaine limite de tension, due à la différence de fonction de travail entre les métaux d'anode et de cathode, augmente pratiquement en fonction du carré de la tension appliquée; ce résultat confirme l'analyse simplifiée de MOTT et GURNEY (1940) et est l'analogue à l'état solide de la loi de puissance à 3/2 pour un courant à charge d'espace limitée dans un vide. Dans cette gamme, le courant varie en fonction de l'inverse cubique de l'épaisseur du cristal et est relativement insensible

aux variations de la température. Entre ces deux courants existe une transition régulière d'un mecanisme de diffusion à un mécanisme d'apport de courant et une cathode virtuelle est établie dans le cristal; il n'existe aucune preuve confirmant l'existence d'une région à résistance négative durant la transition comme le prevoyait SKINNER (1955). Des expressions analytiques simples et exactes sont derivées pour decrire les caracteristiques (courant de sens avant–tension) dans les gammes exponentielles et de loi carrée; elles demontrent que, dépendant principalement de l'épaisseur des cristaux, une haute conductance ou une haute résistance du sens avant peut-être obtenue. Avec une anode de fort verrouillage, le courant à sens inverti est toujours très petit et de très hauts rapports de redressement peuvent être obtenus.

Pour le courant dans la gamme de la loi carrée, le niveau Fermi est presque constant à travers le cristal, exception faite près des contacts de l'anode et de la cathode. Ceci justifie la distinction faite par ROSE (1955) entre les trappes basses qui sont situées au-dessus du niveau Fermi et n'affectent pas la forme des caractéristiques courant–tension et les trappes profondes qui sont situées au-dessous du niveau Fermi et qui modifient sensiblement les caractéristiques courant–tension.

L'article contient des résultats numériques calculés sur la base d'une mobilité d'électron de 1000 cm^2/V-sec, qui est intermédiare entre la valeur de 200 cm^2/V-sec pour le sulfure de cadmium et 9300 cm^2/V-sec pour l'arséniure de gallium. Pour conclure, certaines applications possibles dans les recherches fondamentales de l'état solide sont considérées pour un courant à charge d'espace limitée.

Zusammenfassung—Die Entstehung eines durch die Raumladung begrenzten Stromes in Festkörpern wird behandelt. Als praktisches Beispiel dient ein Material mit einer breiten Energielücke und hohem spezifischem Widerstand, das hochliegende leere Einfangsniveaus enthält, bei dem aber die tiefliegenden leeren Einfangsniveaus durch den von LONGINI und GREEN (1956) beschriebenen Mechanismus der Defektkompensation beseitigt wurden. Ein eindimensionaler Einträger-Strom (Elektron) durch einen Kristall mit parallelen Flächen wird für den Fall eines ohmschen und eines Sperrkontakts behandelt.

Bei kleiner Vorwärtsspannung entsteht der Strom in überwiegendem Masse durch Trägerdiffusion und nimmt mit der Spannung nahezu exponentiell zu. In diesem Bereich ist der Strom stark temperaturabhängig. Bei grosser Vorwärtsspannung entsteht der Strom vorwiegend durch Trägerwanderung. Nach Erreichung einer Spannungsschwelle, die durch den Unterschied der Arbeitsfunktionen der Metalle der Anode und Kathode entsteht, wächst der Strom nahezu mit dem Quadrat der aufgewandten Spannung. Dieses Ergebnis bestätigt die vereinfachte Analyse von MOTT und GURNEY (1940) und entspricht für den Festkörper dem Raumladungsgesetz für einen durch die Raumladung begrenzten Strom im Vakuum. In diesem Bereich ist der Strom der dritten Potenz der Kristalldicke umgekehrt proportional und ist gegen Temperaturveränderung relativ empfindlich. Zwischen beiden Bereichen erfolgt ein glatter Übergang von dem auf Diffusion zu dem auf Trägerwanderung beruhenden Strom, und im Kristall entsteht eine "virtuelle Kathode". Das von SKINNER (1955) postulierte Auftreten eines Gebietes mit negativem Widerstand während des Übergangs liess sich nicht bestätigen. Einfache und genaue analytische Beziehungen liessen sich für vorwärtsgerichtete Strom–Spannungs-Kennlinien für die Bereiche mit exponentiellem und quadratischem Verlauf ableiten. Es ergibt sich, dass je nach der Kristalldicke ein hoher Vorwärtsleitwert oder hoher Vorwärtswiderstand erreicht werden kann. Bei stark sperrender Anode ist der Rückwärtsstrom immer klein, und man kann ein hohes Rektifikationsverhältnis erzielen.

Für Ströme im Bereich des quadratischen Verlaufs ist das Ferminiveau im Kristall nahezu konstant, ausser in der Nähe der Kathoden- und Anodenkontakte. Dies bestätigt die Unterscheidung von ROSES (1955) zwischen hochliegenden Einfangsniveaus, die über dem Ferminiveau liegen und die Gestalt der Strom–Spannungs-Kennlinie nicht beeinflussen, und tiefliegenden Einfangsniveaus, die unterhalb des Ferminiveaus liegen und einen starken Einfluss auf die Strom–Spannungs-Kennlinie ausüben.

Der Artikel gibt numerische Ergebnisse, die unter Annahme einer Elektronenbeweglichkeit von 1000 cm^2/V-sec berechnet wurden. Dieser Wert liegt zwischen dem von 200 cm^2/V-sec für Cadmiumsulfid und 9300 cm^2/V-sec für Galliumarsenid. Zum Abschluss wird die Möglichkeit praktischer Anwendungen des durch Raumladung begrenzten Stromes in der Festkörperforschung erörtert.

NOTATION

b $e^2d^2N_0/\epsilon kT$

B $[\beta I_{2/3}(z)+I_{-2/3}(z)]^2/[\beta I_{-1/3}(z)+I_{1/3}(z)]^2$ or $[\beta J_{2/3}(z)+J_{-2/3}(z)]^2/[\beta J_{-1/3}(z)-J_{1/3}(z)]^2$

d crystal thickness

E electric-field intensity

$\mathscr{E}$ reduced electric-field intensity

e electron charge

g^2 integration constant
i current
$I_\nu(x)$ modified Bessel function
$J_\nu(x)$ Bessel function
J current density
j reduced-current density
k Boltzmann's constant
n density of mobile electrons
n_t density of trapped electrons
N_0 effective integrated density of conduction states
N_t density of trapping states
s reduced distance
s_0 integration constant
T temperature
V inner potential difference
$\mathcal{V}$ reduced inner potential difference
V^a applied potential difference
$\mathcal{V}_a$ reduced applied potential difference
W_f Fermi-level
W_t trap depth
y $\exp[-(U-U_0)/2]$
z $\sqrt{(2)}(js+\alpha^2)^{3/2}/3j$ or $\sqrt{(2)}(-js-\alpha^2)^{3/2}/3j$
α^2 integration constant
β integration constant
ϵ permittivity
θ trapping factor
ϕ work function
ψ electron affinity
μ electron mobility

1. INTRODUCTION

THE conduction of electric current in solids normally takes place by the movement of mobile charge carriers which are already present within the material. The situation most usually encountered is ohmic conduction as in metals where the mobile carriers consist of the valence electrons in the top layers of the Fermi sea. These have a high and uniform density n and a constant mobility μ so that under the influence of an applied field E the drift current density is

$$J_{\text{drift}} = \mu enE \qquad (1)$$

In semi-conductors the mobile carrier density is generally much less than in metals and it is possible for significant non-uniform carrier distributions to exist. In this event the partial pressure of the mobile carriers varies from place to place being greatest where the carrier concentration is greatest. Because of these variations in partial pressure, carriers tend to diffuse into regions of low concentration at a rate proportional to the carrier mobility, to the existing concentration gradient of the carriers and to the mean thermal energy of the carriers. Accordingly, the diffusion-current density along the concentration gradient is

$$J_{\text{diff.}} = \mu kT(-dn/dx) \qquad (2)$$

Since both metals and semiconductors contain mobile charge, it is not possible for an excess charge density to build up within the material. Consequently electrical neutrality is maintained throughout the material and the current-voltage relations are relatively simple. However, experiments by ROSE[1] and by SMITH[2] have shown that transient currents can be observed in high-resistivity materials, and ALFREY and COOKE[3] and RUPPEL[4] have observed steady currents which were very small but which were larger than ohmic currents. Recent experiments in the author's laboratories[5-8] have shown that large, steady currents can be obtained in insulating dielectric crystals which, unlike metals and semiconductors, contain no significant density of thermally generated mobile charge carriers. Current is achieved by injecting electrons from an external source into the conduction band of the crystal and applying an electric field to move the electrons through the crystal. An insulating dielectric crystal provided with an electron-injecting contact (cathode) and an electron-collecting contact (anode) has been termed a "dielectric diode"[7,8]; it is the solid-state analogue of the thermionic vacuum diode.

In this paper a theoretical investigation is made of the steady-state mechanisms of space-charge-limited current in solids. The practical case is taken of a thin, plane, parallel crystal provided with an injecting (ohmic) cathode and a blocking anode. It is shown that, at small forward voltages, current is carried predominantly by carrier diffusion and depends on the applied voltage in an approximately exponential fashion; at large forward voltages current is carried predominantly by carrier drift and has an approximately square-law dependence upon applied voltage. High reverse resistances can be obtained and high rectification ratios are possible.

2. BASIC CURRENT EQUATIONS

Since the case of practical interest is the plane, parallel crystal, we shall consider one-dimensional and one-carrier (electron) current. The interior of the crystal is not electrically neutral and the electron density falls from a high value at the cathode to a low value at the anode so that both electric potential gradients and carrier potential gradients exist. Accordingly the total current density is the sum of drift- and diffusion-current densities and is given by*

$$J = \mu enE + \mu kT\frac{dn}{dx} \tag{3}$$

The cathode contact is placed at the origin of x and the anode contact at $x = d$, where d is the crystal thickness. For forward current the electric potential increases positive as x increases; the forward current is thus negative in sign.

In this case of space-charge-limited (SCL) current, the interior of the crystal is not electrically neutral; current is carried by mobile carriers which are injected from an external source and which form an excess space-charge in the crystal. Consequently, Poisson's equation must be satisfied at all points in the crystal and we have

$$\frac{dE}{dx} = -\frac{en}{\epsilon} \tag{4}$$

The current equation (3) and Poisson's equation (4) may be combined conveniently by eliminating the electron density n to give

$$-J = \epsilon\mu E\frac{dE}{dx} + \frac{\epsilon\mu kT}{e}\frac{d^2E}{dx^2} \tag{5}$$

The various constants which appear in this equation may be eliminated now by changing to the dimensionless variables

$$s = \frac{x}{d};\ \mathscr{V} = \frac{eV}{kT};\ \mathscr{E} = \frac{edE}{kT} \tag{6}$$

$$j = -\frac{e^2d^3J}{\epsilon\mu k^2T^2};\quad b = \frac{e^2d^2N_0}{\epsilon kT} \tag{7}$$

* The negative algebraic signs of electron mobility μ and electron charge e have been taken into account in deriving this equation; accordingly these quantities are now to be regarded as positive numbers.

In these equations the potential difference V is measured with respect to the cathode metal as zero and it should be noted that the reduced potential $\mathscr{V}$ and the reduced current j are both positive for forward current. Making the appropriate substitutions we obtain

$$\frac{d^2\mathscr{E}}{ds^2} + \frac{1}{2}\frac{d\mathscr{E}^2}{ds} - j = 0 \tag{8}$$

This is the basic equation describing SCL current in solids.

In order to use the current equation (3) and Poisson's equation (4) in this way for describing SCL current in solids, the basic problem is simplified to some extent.

All materials possess small amounts of impurities some of which are able to act as donor or acceptor centres and provide mobile charge carriers in the crystal in addition to those injected as space-charge from an external source. If the impurity content is high as in impurity-activated semiconductors then injected space-charge is only significant in the vicinity of the contacts, and in the bulk of the crystal the mobile carrier density is determined predominantly by the density and depth of the impurity centres. In thin crystals or thin layers or under conditions of high current density, however, injected space-charge can become significant as, for instance, in the p–n junction at high forward bias, but this is a situation not normally encountered. If SCL current is to be observed it is preferable for ohmic conductivity due to carriers generated thermally from impurity or valence levels to be small. This requirement can be expressed quantitatively by saying that the dielectric relaxation time of the crystal, $\rho\epsilon$, must be large compared with t_r, the transit time of the injected carriers through the crystal, in order that the injected charge does not decay significantly while in transit. This condition is implied in the equations given since thermal generation of carriers is neglected. These considerations show that fairly wide band-gap materials are necessary if SCL current is to be observed free from ohmic current. The conditions are barely satisfied, for example, by silicon with a band gap of 1·1 eV, an electron mobility of 1200 cm^2/V-sec and an intrinsic resistivity of about 10^5 Ω-cm, but are satisfied, for example, by gallium arsenide with a band

gap of 1·34 eV, an electron mobility of 9300 $cm^2/V\text{-}sec$* and an intrinsic resistivity of about 10^7 Ω-cm.

Empty trapping levels in the crystal are able to reduce the space-charge current considerably because much of the space charge injected into the crystal is immobilized in traps and is unable to contribute to current; the influence of trapping on SCL current has been discussed by ROSE[1]. If the density of initially empty electron traps is N_t at a depth W_t then, when current occurs, the density of filled traps is

$$n_t = N_t/[1 + \exp\{(W_f - W_t)/kT\}]$$

and the ratio of mobile to trapped electrons is

$$n/n_t = N_0[\exp(-W_f/kT) + \exp(-W_t/kT)]/N_t$$

If the traps lie at least several kT above the Fermi-level then

$$n/n_t = N_0 \exp(-W_t/kT)/N_t$$

such traps may be regarded as shallow, and have the property of leaving free a fixed proportion

$$\theta = n/(n+n_t) = N_0/[N_0 + N_t \exp(W_t/kT)]$$

of the space-charge injected into the crystal. Evidently, such traps will reduce the magnitude of the current but, since the ratio of free to trapped charge always remains constant, will not affect the form of the current–voltage characteristics. Their influence may therefore be taken into account simply by defining an effective permittivity $\epsilon\theta$ instead of ϵ in equation (4); this has the effect of reducing the amount of charge in the crystal which is available for carrying current. Traps which lie at least several kT below the Fermi-level may be regarded as deep traps and are able to alter completely the current–voltage characteristics. For such traps the ratio of free to trapped electrons is

$$n/n_t = N_0 \exp(-W_f/kT)/N_t$$

in this case LAMPERT[9] has shown that the proportion of injected space-charge which remains free is extremely small, varies from place to place in the crystal and depends on the magnitude of current.

Although all materials possess donor centres and deep trapping levels to some extent, the experimental evidence suggests that almost complete mutual compensation of these centres can occur under suitable conditions of crystal growth. This has been discussed by LONGINI and GREENE[10], by KAYALI[11] and by ALLEN[12]. LONGINI and GREENE, in particular, show that if the crystal-growing atmosphere contains impurities capable of producing shallow donor centres in the crystal, these can be incorporated in the crystal lattice much more easily if deep empty electron states exist than if such levels are not present. This is because the deep-lying level provides a state of lower energy for the donor electron than does the donor centre itself, thereby reducing the total energy of donor incorporation by an amount $(W_t - W_d)$ where W_t is the depth of the empty level and W_d is the depth of the donor level. Thus, as the crystal grows, with an unavoidable content of deep electron-trapping states formed by thermal defects and acceptor impurities, the simultaneous incorporation of shallow donor impurities ensures that these deep-lying states become filled. Over-compensation is avoided since, as soon as all the deep electron traps are filled, the total energy required for donor incorporation is increased. LONGINI and GREENE show that, in wide band-gap materials in which $(W_t - W_d)$ can be large if the traps are deep and the donors are shallow, compensation is almost exact. Thus, under suitable conditions of crystal growth, shallow donor centres incorporated in the crystal ionize to become shallow traps, and fill deep traps; the result is that residual ohmic conductivity is much reduced and the density of empty deep traps is reduced to the very low level required for large SCL current to be obtained. Thus, in the practical situation, residual ohmic conductivity is negligible and the influence of deep traps has been eliminated, but shallow traps almost certainly do exist. The equations which have been given and the discussion which follows refer to this practical situation.

It is assumed throughout this discussion that thermodynamic equilibrium is maintained at all times between the electron space-charge and the crystal lattice. At small applied electric field strengths this condition is satisfied; the excess

* This is a calculated lattice mobility (H. EHRENREICH, *Prague Conference on Semiconductors, August*, 1960) but present measured values approach this figure.

energy gained from the field by the electrons between collisions with the lattice is much smaller than the mean electron thermal energy and can be satisfactorily dissipated to the lattice at each collision by excitation of acoustic mode vibrations. This is the situation normally existing in semiconductors, for instance, in which the mobile carrier density is sufficiently large that relatively small applied fields are able to produce large current. Under SCL conditions, however, carrier densities are smaller and applied field strengths are greater; conditions are thus more favourable for the mean carrier temperature to rise above that of the crystal lattice. This is likely to occur when the energy gained from the applied field by the individual carrier in moving a mean free path between collisions, becomes comparable with kT and cannot be wholly dissipated by collisions with the lattice. In germanium at room temperature this situation is reached and the carrier mobility begins to decrease when the applied field is of the order of 10^3 V/cm. At higher fields the carriers are able to dissipate excess energy satisfactorily by exciting optical-mode vibrations of the lattice, and the carrier drift-velocity becomes constant and independent of applied field. However, in the wider band-gap, higher-resistivity materials, such as cadmium sulphide and gallium phosphide which are suitable for the observance of SCL current, carrier mobilities are lower and field dependence of mobility should not occur until rather higher field strengths are reached. The experimental evidence for cadmium sulphide indicates that electron mobility remains constant up to field strengths of at least a few times 10^4 V/cm, so that under normal circumstances it seems justified to accept that the electron space-charge remains in thermal equilibrium with the crystal lattice. However, under SCL conditions, field strengths of this order can be exceeded, particularly under pulse or transient operation, and the possible decrease of carrier mobility at the higher applied voltages should be borne in mind. The influence of field dependence of mobility on SCL current in germanium has been discussed by DACEY[13] and in wide band-gap materials, by LAMPERT[14].

A number of previous studies have been made of electron atmospheres and current in insulators. For instance, VON LAUE[15] and FOWLER[16] have discussed conditions in the crystal in the zero-current case in which the Fermi-level remains horizontal through the crystal. More recent studies have been made by SKINNER *et al.*[17,18], WEST[19], MORANT[20] and particularly SKINNER[21] in connexion with the contact charging of insulators. These authors show that the charge transferred into the insulator and the form of the charge distribution in the insulator are controlled largely by the work functions of the contact metals. They distinguish particularly between the case in which all the transferred charge comes from one contact and the electric potential rises steadily through the insulator and the case in which both contacts contribute to the transferred charge and the electric potential has a maximum within the insulator.

The current-carrying case is more difficult to describe. A formal mathematical solution of the basic equation (8) may be obtained readily in terms of Bessel functions.* However, an evaluation of the two integration constants, which is necessary if a useful physical description of current mechanisms is to be obtained, is not possible in explicit form. A simplified treatment of the current-carrying case has been given by MOTT and GURNEY[23] who have considered the situation appropriate to large applied voltages when carrier diffusion can be neglected. These authors show that under these circumstances the SCL current should follow a square-law dependence on applied voltage; this is the solid-state analogue of the three-halves law for SCL current in vacuum. This approach has the merit of simplicity but does not provide an accurate description of current mechanisms particularly near the cathode and anode contacts and is not applicable in the case of small applied voltages. SHOCKLEY[24] has given an approximate discussion of the movement of mobile carriers over a potential maximum, and SHOCKLEY and PRIM[25] give a more accurate discussion of the same case. These authors simplify the problem by considering current in a crystal of undetermined extent and by assuming that, at large distances, drift mechanisms become predominant so that the approximate solution derived by MOTT and GURNEY is obtained. This approach provides a useful account of physical conditions in the crystal for the case of

* A first integration of equation (8) gives a particular form of Riccati's equation; this is discussed by MCLACHLAN[22].

large currents in which a potential maximum does exist in the crystal. However, it cannot be used to discuss current mechanisms at small or large applied voltages, to discuss physical conditions near the cathode or anode contacts, or to provide an account of current–voltage characteristics.

Current mechanisms in a finite crystal bounded by metallic electrodes have been discussed by SKINNER[26]. This author shows that the current–voltage characteristics are influenced markedly by the nature of the electrodes; in particular, the expected rectification characteristics are obtained if the work function of the cathode and anode used by these authors is complex and does not provide a description of physical conditions in the crystal, of current mechanisms, or a usable account of current–voltage characteristics.

The present paper is an attempt to provide a clear and useful description of SCL current in solids. In particular the two integration constants which arise in the formal mathematical solution of equation (8) are evaluated in a manner which enables the underlying physical processes to be kept in mind. Before discussing the current-carrying case, however, it is appropriate to review briefly the zero-current case, since this enables a

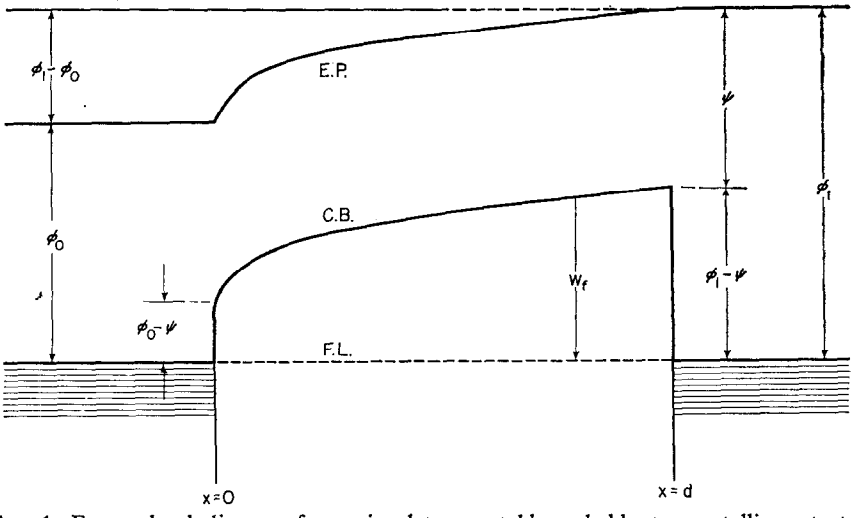

FIG. 1. Energy-level diagram for an insulator crystal bounded by two metallic contacts of unequal work functions. The variations of electric potential, conduction-band level, and Fermi-level are shown respectively by the lines marked E.P., C.B. and F.L. Electric potential is measured positive downwards. ψ = electron affinity of crystal; ϕ_0 = work function of cathode metal; ϕ_1 = work function of anode metal; $\phi_0-\psi$ = cathode potential step eV_0; $\phi_1-\psi$ = anode potential step eV_1; $\phi_1-\phi_0$ = contact potential difference between cathode and anode metals. (W_f = Fermi-level measured downwards from conduction band.)

metals are different. A further and most interesting result is the predicted existence of a negative-resistance region in the current–voltage characteristics. The particular case when cathode and anode metals are identical has been treated by SUITS[27]. In this case no rectification is obtained; the current is proportional to voltage at low applied voltage, but, if space charge is significant, follows a square-law dependence on voltage at high applied voltage. Unfortunately the approach clearer understanding of current mechanisms to be obtained.

3. ZERO-CURRENT CASE

When an insulator which contains no appreciable density of mobile electrons is placed in contact with a metal, electrons diffuse into the insulator until the space-charge field set up in the insulator is sufficient to balance the diffusion of electrons from the metal. The equilibrium situation is

illustrated qualitatively in Fig. 1 which shows the energy-level diagram for an insulator crystal bounded by two metallic contacts. The variation of electric potential through the system is also shown; this is to illustrate in particular that there is no discontinuity of potential at the ideal contact. In this and all subsequent energy-level diagrams the electron energy is measured positive upwards and electric potential is therefore measured positive downwards. The curvature of the conduction band of the crystal near the contact with the metal of lower work function is caused by the space-charge field of the electrons which have diffused from the metal. The Fermi-level in the crystal is measured downwards from the conduction band of the crystal; this is mainly for convenience in the current-carrying case discussed subsequently. For generality we have taken the case in which the contact metals have different work functions. Since the greater charge is transferred into the crystal at the contact with the metal of the lower work function, it is evidently appropriate to take this metal as the cathode.

In equilibrium, the diffusion of electrons away from the contact is balanced by the drift of electrons toward the contact. Accordingly we may put j equal to zero in equation (8) when a first integration gives

$$\frac{d\mathscr{E}}{ds}+\frac{\mathscr{E}^2}{2}=g^2 \tag{9}$$

In this expression g^2 is an integration constant. Under zero-current conditions there is no potential difference between anode and cathode and the Fermi-level is horizontal throughout the insulator crystal. Consequently the density of electrons in the conduction band at any point in the crystal is given by

$$n=N_0\exp(-W_f/kT)=N_0\exp(eV/kT)=N_0e^{\mathscr{V}} \tag{10}$$

Using equations (6) we have

$$\mathscr{E}=-\frac{d\mathscr{V}}{ds};\quad \frac{d\mathscr{E}}{ds}=-be^{\mathscr{V}} \tag{11}$$

so that equation (9) gives for the electric-field intensity

$$\mathscr{E}=\pm(2be^{\mathscr{V}}+2g^2)^{1/2} \tag{12}$$

The appropriate sign to be used in this equation depends on the sign of the electric-field intensity. From equation (12) we obtain for the electric potential

$$\exp(\mathscr{V}-\mathscr{V}_0)=\frac{\sinh^2(g^2/2)^{1/2}s_0}{\sinh^2(g^2/2)^{1/2}(s+s_0)} \tag{13}$$

In these equations the quantity eV refers, as usual, to the total energy of the electron. It is not usually necessary or desirable to separate the thermal and electric components of the total energy, but it should be borne in mind that the potential steps eV_0 and eV_1 at the contacts are not necessarily caused by a change of electric potential. This is of relevance when considering boundary conditions. The Fermi-level of the system, in particular the Fermi-level of the cathode metal, is a convenient level from which to measure the electron energy and if this is done the actual electric potential in the crystal relative to the cathode metal is

$$V+(\phi_0-\psi)/e=V-V_0$$

Now the integration constants g^2 and s_0 can be found from the equilibrium boundary conditions on the electron-charge density at the contacts; at cathode and anode we have respectively

$$\mathscr{V}_0=eV_0/kT=-(\phi_0-\psi)/kT$$

and

$$\mathscr{V}_1=eV_1/kT=-(\phi_1-\psi)/kT$$

Unfortunately the constants cannot be expressed explicitly in terms of the boundary conditions and it is therefore necessary to derive approximate expressions.

Consider the case when $\mathscr{V}_0$ is small (ohmic or injecting cathode) and $\mathscr{V}_1$ is large (blocking anode) which is the case to which this paper particularly refers. The electron density in the crystal at the cathode contact is large under these circumstances, but it must evidently decrease rapidly further into the crystal; if this were not so then large amounts of charge could be transferred into the crystal and this is contrary to the observed effects of contact charging of insulators. Thus $d\mathscr{E}/ds$ is significant only near the contact, and consequently the term $2b\exp\mathscr{V}$ in equation (12) is negligible except near the contact. Now $\mathscr{E}\simeq\mathscr{V}_1-\mathscr{V}_0$, so we conclude that the integration constant g^2 is large and positive. Combining now equations (10) and (13), it is evident that s_0 must be small if the electron density is to decrease rapidly away from the contact. Using that g^2 is large and s_0 is small,

equation (13) for the potential may be approximated in the vicinity of cathode and anode respectively and we obtain, to a first approximation,

$$s_0^2 = 2\exp(-\mathscr{V}_0)/b \qquad (14)$$

$$\sqrt{(2)}g = -[\mathscr{V}_1 + \log(b/2\mathscr{V}_1^2)] \qquad (15)$$

It should be remembered that $\mathscr{V}_0$ and $\mathscr{V}_1$ in these equations are negative.

The smallest value which can be used for eV_0 without becoming involved in electron degeneracy is obtained from equation (13) and is shown in Fig. 2. The following typical physical parameters have been used: crystal thickness $d = 10\,\mu$; temperature $T = 300°\text{K}$; $eV_0 = 0{\cdot}1$ eV. Various values of eV_1 have been taken appropriate to the cases of a blocking anode (g^2 positive, $eV_1 = 1{\cdot}0$ eV); a semi-infinite crystal (g^2 zero, $eV_1 = 0{\cdot}472$ eV which is the potential at a distance of $10\,\mu$ into a semi-infinite crystal); and an injecting anode (g^2 negative, $eV_1 = 0{\cdot}1$ eV). The integration constants g^2 and s_0 for the latter two cases can be ob-

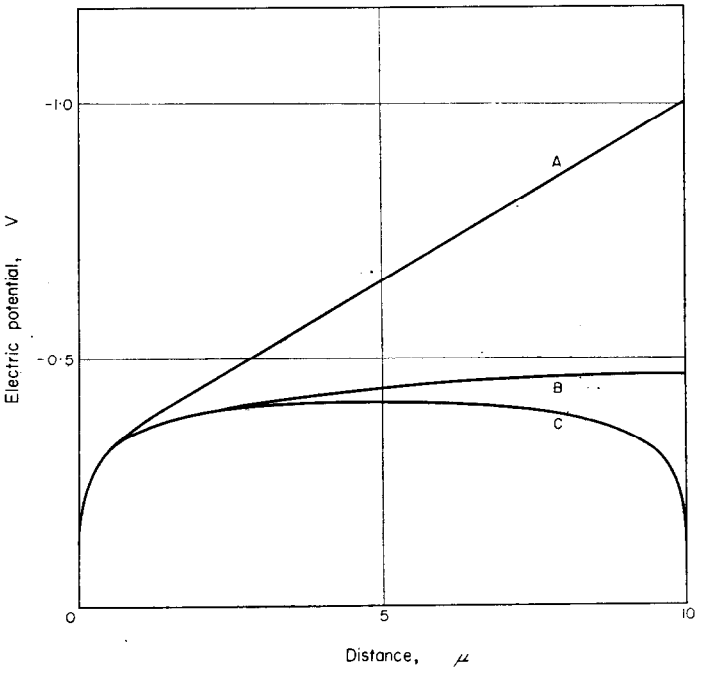

FIG. 2. Variation of conduction band through the crystal for the zero-current case. The zero of reference is the Fermi-level of the cathode metal. Cathode potential step $eV_0 = 0{\cdot}1$ eV; anode potential step $eV_1 = 1{\cdot}0$ eV (curve A), $0{\cdot}472$ eV (curve B) and $0{\cdot}10$ eV (curve C).

at the cathode is about $0{\cdot}1$ eV, and a suitable value of eV_1 to provide a blocking contact is $1{\cdot}0$ eV. It is unlikely of course that eV_0 would be as small as this at a normal contact between a metal and an insulator. However, by suitable formation of the cathode contact it is possible to arrange for the effective value of eV_0 to be small; this is done in the dielectric diode in order that SCL current may be achieved.

The variation of electric potential in the crystal tained by arguments similar to those used for the case of the blocking anode. In this connexion one finds references in the literature[19,21] to the existence of three solutions to the basic zero-current equation. This is unnecessarily confusing; there is only one solution but this transforms from hyperbolic to logarithmic and then trigonometric form according as the integration constant g^2 is positive, zero or negative. However, the diagram shows well that conditions near the cathode are not much

influenced by the nature of the anode. It is also apparent that the injected charge density decreases very rapidly at small distances into the crystal so that most of the injected charge lies within the surface layers of the crystal.

These various forms of electron atmosphere have been discussed in some detail by SKINNER[21] and will not be considered further here since our main interest is in the current-carrying case.

4. CURRENT-CARRYING CASE

The discussion given above of zero-current conditions in the insulator crystal is very useful for visualizing qualitatively the conditions obtaining when current occurs. In this connexion the variation of electric potential and electric field intensity through the crystal are shown qualitatively in Fig. 3 for the particular case of an ohmic cathode contact and a blocking anode contact. For zero current the potential rises steadily and the electric field falls steadily as shown by the full lines. When a positive voltage is applied to the anode, however, electrons are drawn from the cathode space-charge and travel through the crystal towards the anode so that forward current occurs; conditions are now qualitatively as shown by the broken lines. The electron potential energy has a maximum near the cathode which acts as a "virtual cathode" for the emission of electrons into the crystal; this is analogous to the virtual cathode which exists in the thermionic vacuum diode. Up to this point the electron potential energy rises positive like the zero-current case, but beyond this point it falls rapidly, passes through zero and increases negative towards the anode. The electric-field intensity will pass through zero at the position of the virtual cathode and will then increase negative towards the anode.

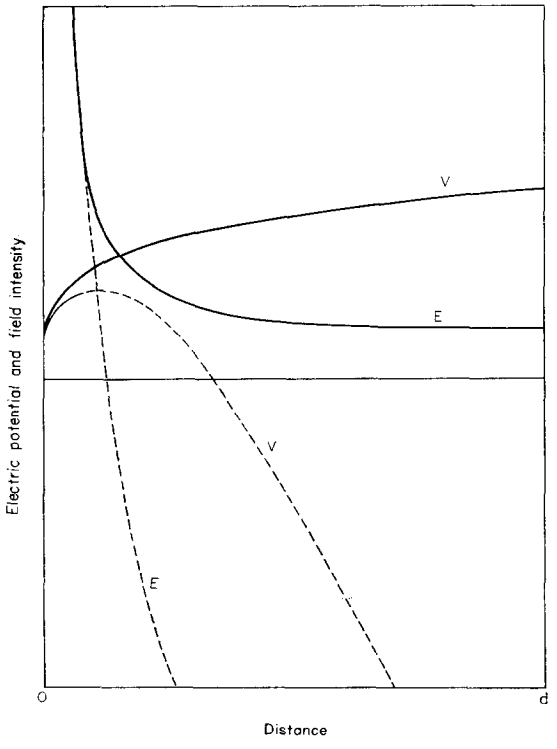

FIG. 3. A qualitative illustration of the variation of electric potential V and field intensity E through an insulator crystal for the zero-current case (full lines) and the current-carrying case (broken lines).

With this diagram in mind we may return to discuss the basic equation (8). The formal mathematical solution will first be given and the appropriate boundary conditions then discussed.

A. *Formal mathematical solution*

The current density is constant throughout the crystal; consequently equation (8) may be integrated directly to give

$$\frac{d\mathscr{E}}{ds}-\frac{\mathscr{E}^2}{2}-(js+\alpha^2)=0 \tag{16}$$

The quantity α^2 is a constant of integration. At this stage the algebraic sign and numerical magnitude of α^2 are not known; consequently it is not known whether the quantity $(js+\alpha^2)$ is positive or negative. However, if we now change the variables by writing

$$\log y=\tfrac{1}{2}\int_0^s \mathscr{E}\,ds=-\frac{\mathscr{V}-\mathscr{V}_0}{2} \tag{17}$$

$$z=\frac{\sqrt{(2)}}{3j}(js+\alpha^2)^{3/2}+i\frac{\sqrt{(2)}}{3j}(-js-\alpha^2)^{3/2} \tag{18}$$

we may select the real part of z if $(js+\alpha^2)$ is positive and the imaginary part of z if $(js+\alpha^2)$ is negative. The discussion will be continued on the assumption that this quantity is positive and will be transformed as necessary if it should be negative.

Making the substitutions we obtain

$$\frac{d^2y}{dz^2}+\frac{1}{3z}\frac{dy}{dz}-y=0 \tag{19}$$

This equation has the solution

$$y=\text{const.}\times z^{1/3}[\beta I_{-1/3}(z)+I_{1/3}(z)] \tag{20}$$

where β is a second constant of integration. By taking $(js+\alpha^2)$ positive and using the real part of z, the solution has been obtained in terms of Bessel I functions rather than in terms of J functions. This seems more appropriate, since the I functions are non-oscillatory and conditions in the crystal must evidently be non-oscillatory. The constant serves to determine the absolute level of potential and is fixed as soon as the reference zero of potential is decided on. As in the zero-current case, the Fermi-level of the cathode metal will be taken as the zero of electron energy. The electric potential difference

$$(V-V_0)=(kT/e)(\mathscr{V}-\mathscr{V}_0)$$

between any point in the crystal and the cathode metal is then given by

$$\exp(\mathscr{V}-\mathscr{V}_0)=\left(\frac{z_0}{z}\right)^{2/3}\left[\frac{\beta I_{-1/3}(z_0)+I_{1/3}(z_0)}{\beta I_{-1/3}(z)+I_{1/3}(z)}\right]^2 \tag{21}$$

The electric-field intensity in the crystal is given by $\mathscr{E}=2d(\log y)/ds$ from which

$$\mathscr{E}=[2(js+\alpha^2)]^{1/2}\left[\frac{\beta I_{2/3}(z)+I_{-2/3}(z)}{\beta I_{-1/3}(z)+I_{1/3}(z)}\right] \tag{22}$$

The density of electrons in the crystal is given by $bn/N_0=-d\mathscr{E}/ds$ from which

$$\frac{bn}{N_0(js+\alpha^2)}=\left[\frac{\beta I_{2/3}(z)+I_{-2/3}(z)}{\beta I_{-1/3}(z)+I_{1/3}(z)}\right]^2-1 \tag{23}$$

The discussion which follows becomes much less cumbersome if we now define the quantity B by

$$B=\left[\frac{\beta I_{2/3}(z)+I_{-2/3}(z)}{\beta I_{-1/3}(z)+I_{1/3}(z)}\right]^2 \tag{24}$$

so that we may write for the electric-field intensity

$$\mathscr{E}=[2(js+\alpha^2)B]^{1/2}=[2(js+\alpha^2)+2bn/N_0]^{1/2} \tag{25}$$

and for the electron density

$$bn=N_0(js+\alpha^2)(B-1) \tag{26}$$

To proceed further it is necessary to evaluate the integration constants α^2 and β. This can be done through proper choice and utilization of boundary conditions

B. *Boundary conditions*

Under zero-current conditions the electron atmosphere in the crystal is in thermodynamic equilibrium throughout with the electron atmospheres in cathode and anode metals. In particular this is true in the crystal at the actual cathode and anode surfaces. This circumstance was used to provide the boundary conditions for the zero-current case, and the same boundary conditions may be used for the current-carrying case.

Consider first the cathode contact. The cathode metal acts as an effectively infinite reservoir of electrons, and any practical current will not appreciably affect the equilibrium electron atmosphere at the actual cathode contact itself. Thus in the surface of the crystal in contact with the cathode metal, the electron density will always remain constant and equal to $n_0=N_0\exp\mathscr{V}_0$. In the vicinity of the cathode the electron density is large; consequently drift- and diffusion-current tendencies are large. When forward current occurs the diffusion-current tendency becomes larger than the drift-current tendency and we may consider that, near the cathode, forward current is carried by diffusion.

At the anode contact conditions are rather different. When current occurs, electrons move through the crystal towards the anode and evidently the electron density increases considerably over most of the crystal. However, any practical current will not appreciably disturb the equilibrium electron atmosphere in the anode metal, and at the actual anode contact the electron density will remain constant and equal to $n_1=N_0\exp\mathscr{V}_1$. In effect, and because $\mathscr{V}_1$ is large, the anode metal acts as a sink for electrons. Thermal equilibrium will not be reached in the anode metal, of course, over a distance of the order of a collision mean free path, but this is so small compared with any practical crystal thickness that it is quite permissible to assume equilibrium conditions to exist at the actual anode contact. The consequence of this is that in

the crystal near to the anode the electron density falls off very rapidly to the very small value n_1 at the actual anode contact. Near the anode, therefore, there is a large concentration gradient of electrons. Since the electric field cannot change very much over this region, whereas the electron density falls considerably, it is evident that near the anode as well as near the cathode forward current is carried by diffusion.

In the ideal contact, the energy steps eV_0 and eV_1 are due entirely to the discontinuity in the type of crystal lattice which results in a different energy system on either side of the contact. This is the situation, which has been illustrated in Fig. 1, which shows a discontinuity of electron energy at the contacts, although there is no discontinuity of electrostatic potential. In any real contact, however, the situation may be modified by the existence of surface states for electrons and by surface contamination.

Surface states can arise in a variety of ways and it is not possible to do more than make a qualitative estimation of their effects. Tamm surface states will arise at the surface of the free crystal because of the abrupt discontinuity in the periodic potential of the crystal lattice. SHOCKLEY[28] has considered the circumstances under which surface states originate from valence levels and concludes that in this case each surface atom gives rise to one surface state and that these states are half occupied. Discussions of this sort based on the simplified model of a semi-infinite one-dimensional crystal are useful for visualizing qualitatively the situation in a real crystal, and it seems certain that surface states do exist. In semiconductors, for instance, in which the surface charge is compensated by the underlying fixed space-charge of ionized donors or acceptors, BARDEEN[29] has shown that surface states can play a significant part in establishing contact potentials. However, in wide band-gap insulator-type materials in which the Fermi-level lies far from conduction or valence levels, no appreciable curvature of the electron-energy levels near the surface can be caused in this way. Nevertheless, if the crystal surface possessed a high density of empty states, it is presumable that on contact with a metal there could be sufficient transfer of electrons to these to set up a significant space-charge layer of atomic thickness in the crystal surface. The rise of electric potential through this layer would introduce an electrostatic component into the energy step at the contact.

In all real contacts the situation is modified by impurity atoms or molecules adsorbed on to the surface before contact. These surface layers prevent intimate contact between metal and crystal and, moreover, if the ionization potential of the absorbed impurity is lower than the work function of the underlying material so that there is a tendency for electron exchange to occur by ionization of the impurity, or if the adsorbed impurity has a strong electron affinity and so is able to accept an electron from the underlying surface, then an electric dipole layer may be set up at the surface which, as before, would introduce an electrostatic component into the potential-energy step at the contact. A situation similar to this is deliberately produced in the dielectric diode.[6] Here the cathode energy step is made very small by introducing a high density of shallow donor centres into the surface layers of the crystal so that a very thin electric double layer is produced at the cathode contact. This is sufficiently thin as to be transparent to electrons which penetrate the resultant electric potential spike by quantum-mechanical tunnelling.[30] The result is that the conduction band of the crystal at the cathode contact is brought down near to the Fermi-level of the cathode metal; the zero-current inner potential difference across the crystal is now $(\phi_1-\psi-w)/e$, where w is the Fermi-level in the crystal in the highly doped surface layers, instead of $(\phi_1-\phi_0)/e$.

Provided that any potential hump produced in these ways between metal and crystal is very thin, as it will be since adsorbed surface layers are generally only of atomic thickness and electrons in surface states are effectively localized at the surface, the electron atmospheres on each side of the contact will remain in thermal equilibrium although the over-all effective energy step for the contact will not be the true value for the ideal contact. Accordingly, it is quite justifiable to consider that the over-all effect of the contact is to produce an energy step and that the electron atmospheres on either side of the contact remain in thermal equilibrium, although the magnitude eV of the energy step will not necessarily be equal to $(\phi-\psi)$ the true difference between the work function of the metal and the electron affinity of the crystal.

Using these boundary conditions on the electron

density we can in principle obtain the integration constants from equation (23) for the electron density.

In this way we obtain

$$-\beta = \frac{I_{-2/3}(z_0)-(\pm)\sqrt{(B_0)}I_{1/3}(z_0)}{I_{2/3}(z_0)-(\pm)\sqrt{(B_0)}I_{-1/3}(z_0)} \quad (27a)$$

$$-\beta = \frac{I_{-2/3}(z_1)-(\pm)\sqrt{(B_1)}I_{1/3}(z_1)}{I_{2/3}(z_1)-(\pm)\sqrt{(B_1)}I_{-1/3}(z_1)} \quad (27b)$$

where the subscripts 0 and 1 refer respectively to cathode and anode conditions. Either of these equations provides the value of β; by eliminating β between them, the equation defining α^2 is obtained. However, there is an ambiguity in these equations for α^2 and β, since it is not known whether the positive or negative sign is required for $\sqrt{(B)}$. This ambiguity may be resolved by using the fact, from equation (25), that the sign of $\sqrt{(B)}$ is the same as the sign of the electric-field intensity. Consequently the sign required depends on whether cathode or anode conditions are being discussed and on the magnitude and direction of current.

Using these results we may proceed to discuss current mechanisms.

5. CURRENT MECHANISMS IN THE RECTIFYING DIELECTRIC DIODE

For a discussion of the current-carrying case we shall take the practical situation of a crystal provided with an ohmic cathode (n_0 large) and a blocking anode (n_1 small). The forward current case is the more interesting and will be considered first; reverse characteristics will be discussed subsequently.

A. *Forward-current case*

At small applied voltages current is carried predominantly by diffusion and, except at very small currents, follows an approximately exponential dependence upon applied voltage.

(a) *Exponential current range.* When a small forward voltage is applied the current is sufficiently small that conditions in the crystal near the cathode are not very different from the zero-current case. Thus equation (16) should describe conditions which are not very different from zero-current conditions. This shows that for small current $\alpha^2 \simeq g^2$ and, since the maximum value of s is unity, that $j \ll \alpha^2$. Accordingly the quantity $(js+\alpha^2)$ is positive over the whole range of s from cathode to anode. This means that z is positive and real over the whole range of s so that Bessel I functions may be used throughout. Further, since we are considering small currents, z is large and the asymptotic expansions for the I functions may be used throughout. The electric-field intensity remains positive from cathode to anode; consequently the positive sign is required for $\sqrt{(B)}$ in the evaluation of the integration constants.

For small currents, therefore, and to the degree of accuracy required, equation (27) can be expressed

$$-\beta = \frac{\{\sqrt{(B)}-1+[7+5\sqrt{(B)}]/72z\}e^z-[\sqrt{(B)}+1](\cos\pi/6)e^{-z}}{\{\sqrt{(B)}-1+[7+5\sqrt{(B)}]/72z\}e^z+[\sqrt{(B)}+1](\cos\pi/6)e^{-z}} \quad (28)$$

Since z is very large, it is apparent that $-\beta$ is almost equal to unity; it is in fact just less than unity. However, the slight deviation of $-\beta$ from unity is significant, because in equation (21) for the electric potential we are concerned with the very small difference between two Bessel I functions which are extremely large and almost equal in magnitude. Introducing cathode and anode conditions in turn into this equation, equating the two results, and using that $B_1 \simeq 1$, $B_0 \gg 1$ and $z_0, z_1 \gg 1$, we obtain

$$\exp[-2(z_1-z_0)] = \{[\sqrt{(B_1)}-1]/2+1/12z_1\}\times \times[\sqrt{(B_0)}+1]/[\sqrt{(B_0)}-1] \quad (29)$$

This result is valid provided $72z_0 \gg 5\sqrt{(B_0)}$, which is certainly true for small currents. These two equations (28) and (29) may be used to provide the integration constants α^2 and β and hence to obtain a description of physical conditions in the crystal.

The electric potential in the crystal is obtained from equation (21). Using the asymptotic expansions of the Bessel I functions together with the value of β given by equation (28), we obtain

$$\exp(\mathscr{V}-\mathscr{V}_0)=\frac{\sinh^2\{z_1-z_0+\frac{1}{2}\log[(B_1-1)/4+1/12z_1]\}}{\sinh^2\{z_1-z+\frac{1}{2}\log[(B_1-1)/4+1/12z_1]\}} \tag{30}$$

For the particular case of zero current this reduces to equation (13) previously derived for zero-current conditions.

In order to obtain the current–voltage characteristics of the crystal, we put $z=z_1$ in equation (30). Using equation (29) this then gives

$$\exp(\mathscr{V}_a-\mathscr{V}_0)=\frac{B_1-1}{B_0-1}+\frac{1}{3z_1(B_0-1)} \tag{31}$$

In this result $\mathscr{V}_a-\mathscr{V}_0$ is the reduced inner potential difference across the crystal; this is the reduced potential difference between the cathode surface of the crystal and the anode surface of the crystal.

It follows that

$$-J=\sqrt{(2)}\alpha n_1\mu kT[\exp(eV_a'/kT)-1]/d \tag{32}$$

In this equation V_a denotes the external applied voltage between cathode and anode metals (external voltages will be dashed throughout to distinguish them from inner potentials). This result implies the rectifying action of the diode although it is strictly valid only for small forward current. Provided that the quantity α^2 does not vary rapidly, it is evident that the current increases approximately exponentially with the applied voltage. This is a useful result for the thinner crystals and thin insulating layers ($d<1\,\mu$) in which current of practical magnitude can be reached at applied voltages small enough that carrier-diffusion mechanisms remain predominant.

For very small currents, conditions in the crystal will not be very different from zero-current conditions, and we may write $\alpha^2=g^2$. This is consistent with equation (29) which then reduces to the zero-current case provided the current is sufficiently small that $1/12z_1\ll[\sqrt{(B_1)}-1]/2$. This condition requires that $j\ll\sqrt{(2)}gb/N_0$; thus equation (32) can be used with $\alpha^2=g^2$ only if $eV_a'\ll kT$ so that

$$-J=\sqrt{(2)}g\mu en_1V_a'/d \tag{33}$$

For larger but still small currents so that we still have $j\ll\alpha^2$ it is evident, as the current increases, that z_1 becomes smaller and eventually $1/12z_1\ll[\sqrt{(B_1)}-1]/2$. Equation (29) now reduces to

$$j\exp[\sqrt{(2)}\alpha]=4\sqrt{(2)}\alpha \tag{34}$$

This equation provides the value of α^2 to be used in equation (32) when $\sqrt{(2)}gb/N_0\ll j\ll\alpha^2$. By examination of this equation it is found that the largest value of j for which a solution is possible is $j=2{\cdot}68$ corresponding to $\alpha^2=4{\cdot}47$. Using these corresponding values of j and α^2, it is apparent that the requirement $j\ll\alpha^2$ is not satisfied. Accordingly, it is not safe to consider that the exponential current range extends up to values of j greater than unity.

For smaller values of j the solution of equation (34) has two branches, one of which provides decreasing values of α^2 as j decreases while the other provides increasing values of α^2. Considering the decreasing branch first, it is found that it is never possible to have $j\ll\alpha^2$, as required in the small current range. Thus this branch of the solution is not consistent with the original equations and may be disregarded. Considering now the increasing branch it is found that α^2 increases slowly as j decreases and except for values of j near unity, it is true that $j\ll\alpha^2$. This branch may therefore be accepted and we have that the exponential current range lies within the limits $\sqrt{(2)}gb/N_0\ll j<1$.

In the exponential current range discussed here the electric field intensity has remained positive throughout the crystal from cathode to anode. This follows from equation (25), since $j\ll\alpha^2$. Consequently current occurs against the direction of the electric field. Thus the diffusion-current tendency is everywhere greater than the drift-current tendency, and current takes place by diffusion. When the applied voltage is large, however, so that $eV_a'\gg kT$, the drift-current tendency is larger than the diffusion-current tendency. Thus between the small-current and large-current ranges a transition occurs from a predominant diffusion mechanism to a predominant drift mechanism. The current range over which this occurs may be termed the transition range and is discussed below.

(b) *Transition-current range.* As the current rises

through the exponential current range, z_0 and z_1 are decreasing; when j is approaching unity α^2 is quite small and z_0 and z_1 have decreased to quite small values. Accordingly, in the transition-current range it is not possible to use the asymptotic expansions of the Bessel functions. The integration constants α^2 and β cannot be evaluated explicitly and a quantitative account of current mechanisms in this range cannot be given easily. However, it is in this range that the current mechanism changes from being predominantly carrier diffusion to predominantly carrier drift and it is in this range that the negative-resistance characteristics predicted by SKINNER should be found. Thus it is of value to discuss the transition range in some detail in order to obtain an understanding of the physical processes involved.

First we may consider the behaviour of the integration constant α^2. Turning to equation (16) we may write this in the form

$$\mathscr{E}^2 = 2(js+\alpha^2)-2\,d\,\mathscr{E}/ds \qquad (35)$$

Now MOTT and GURNEY[23] have shown that, if the space-charge equations are solved on the basis of a drift-current mechanism alone, $\mathscr{E} = -(2js)^{1/2}$. Electron diffusion does exist, however, and assists forward current. Thus if diffusion mechanisms are taken into account the electric field existing for a given current will be smaller than required on the basis of a drift mechanism alone. Since the quantity $d\mathscr{E}/ds$ is negative, it follows that the quantity α^2 becomes negative in the large-current range and is numerically larger than $d\mathscr{E}/ds$. An estimate of the numerical magnitude of α^2 in the large-current range may thus be obtained from equation (4) which gives $d\mathscr{E}/ds = -bn/N_0$. On the basis of a drift mechanism alone the space-charge capacitance of the diode is $3\epsilon A/2d$ giving that the mean space-charge density of electrons is $3\epsilon V_a'/2ed$ where V_a' is the applied voltage. Combining these estimates we conclude that the average value of $d\mathscr{E}/ds$ is of the order of $3eV_a'/2kT$ showing that, for large currents where the applied voltage is certainly greater than unity, we have $-\alpha^2 > 10^2$. This is only a very rough estimate of the magnitude of α^2 but it is sufficient for our present purpose. We conclude therefore that in the transition-current range the quantity α^2 continues to decrease positive, passes through zero and then becomes large and negative.

For the particular case of $\alpha^2 = 0$ we have $z_0 = 0$ and equation (27a) for β simplifies to give $\beta \simeq 0$. Using this value of β in equation (27b) with $\sqrt{(B_1)} \simeq 1$ we find $z_1 = 1{\cdot}04(2)$. The slight deviation of β from zero and $\sqrt{(B_1)}$ from unity does not affect this result significantly. We thus have $j = 4{\cdot}88$ to provide a first fixed point in the transition current range. Using that $\beta \simeq 0$, $z_0 = 0$, we find from equation (21) that for this value of j the inner potential across the crystal is given by

$$\exp(\mathscr{V}_a - \mathscr{V}_0) = 2\beta^2/[z^{1/3}\Gamma(\tfrac{2}{3})I_{1/3}(z_1)]^2 \qquad (36)$$

When the current is sufficiently large that α^2 has passed through zero and become negative, the imaginary part of z is required [from equation (18)] in the cathode regions of the crystal where s is small enough that numerically $js < \alpha^2$. Under these conditions equation (19) transforms to

$$\frac{d^2y}{dz^2} + \frac{1}{3z}\frac{dy}{dz} + y = 0 \qquad (37)$$

and equations (21–24) for the electric potential, electric-field intensity, electron density and the quantity B, respectively, must be expressed in terms of Bessel J functions instead of I functions.

Since α^2 remains negative for large currents, it is apparent that conditions in the cathode regions of the crystal must be described in terms of the imaginary part of z through the remainder of the transition range and for large currents.

Now we have seen that for large currents the electric field at the anode has passed through zero and become negative. Equation (25) shows that $\mathscr{E}_1$ can become zero only if the quantity B_1 becomes zero which requires that $(j+\alpha^2) = -bn_1/N_0$. Thus while the electric field at the anode is near zero the quantity $(j+\alpha^2)$ is negative and numerically very small; under these circumstances the situation is described in terms of Bessel J functions throughout the whole crystal. Using that $(j+\alpha^2)$ and therefore z_1 are very small while $\mathscr{E}_1$ is near zero, the equations for β can be simplified and the behaviour of this integration constant followed. The detailed examination is lengthy and is therefore omitted, but the interesting result is that β possesses a singularity just before $\mathscr{E}_1$ becomes zero. This is illustrated in Fig. 4, which shows the behaviour of the integration constants α^2 and β through the transition-current range. As the anode

electric field goes to zero, β rapidly increases large and positive and finally becomes positive and infinite; it then changes sign and returns from negative infinity as the anode electric field passes through zero and increases negative. At this singularity of β the electric field at the anode changes sign, and drift mechanisms now begin to assist the forward diffusion current. Accordingly it is convenient to regard this as the point of transition from a predominant-diffusion mechanism of current to a predominant-drift mechanism.

This discussion of the transition range has equation (23) together with the relation $n = N_0 \exp(-W_f/kT)$ and is also shown in the figure. These curves refer to a crystal 1 μ thick at a temperature of 300°K. A typical value of $\epsilon = 10^{-10}$ F/m has been used for the permittivity of the crystal (dielectric constant $\kappa = 11$) and the electron mobility has been taken as 0·1 m²/V-sec (1000 c.g.s. units) which is intermediate between the value 0·02 m²/V-sec for cadmium sulphide and 0·9 m²/V-sec for gallium arsenide.

In order to make this diagram more useful the potential variation and Fermi-level for zero current

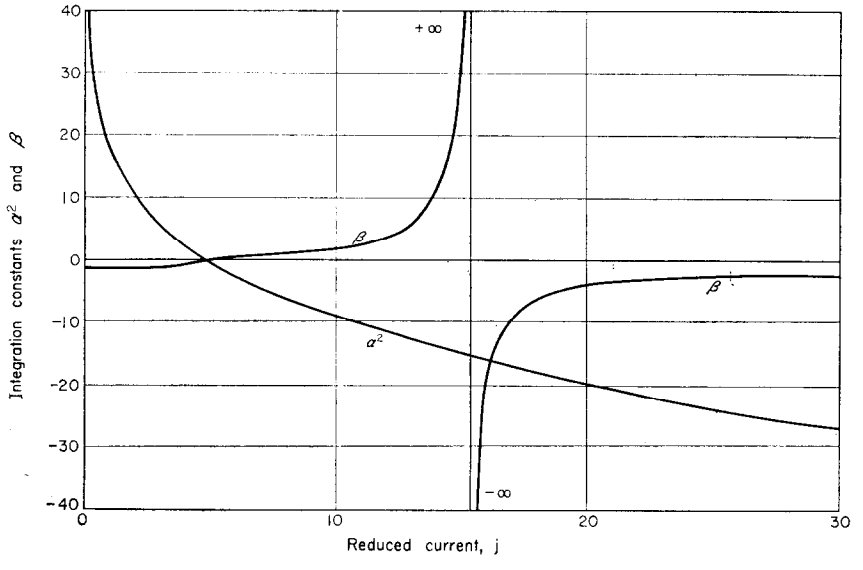

FIG. 4. Dependence of the integration constants α^2 and β upon the magnitude of the reduced-current density j through the transition-current range. The singularity of β marks the transition from a predominant-diffusion mechanism of current towards a predominant-drift mechanism.

shown that, for the particular case when $\alpha^2 = 0$, a fixed point can be established at which corresponding values of the integration constants and of the current and applied voltage can be evaluated. This can also be done and a second fixed point established for the particular case when $|\beta| = \infty$ although the detailed derivation of each has been omitted for brevity. However, the potential variation through the crystal for each of these points has been calculated from equation (21) and is illustrated in Fig. 5. The position of the Fermi-level in the crystal has been calculated using and for a current above the transition range are also shown. The values of the integration constants for the latter case have been evaluated as described in the next sub-section. It is interesting to observe from this diagram how physical conditions in the crystal alter as the current mechanism changes from being predominantly carrier diffusion to predominantly carrier drift. In particular, as the current increases from zero through the exponential and transition-current ranges and the electron space-charge spreads into the crystal from the cathode there is very little movement of the

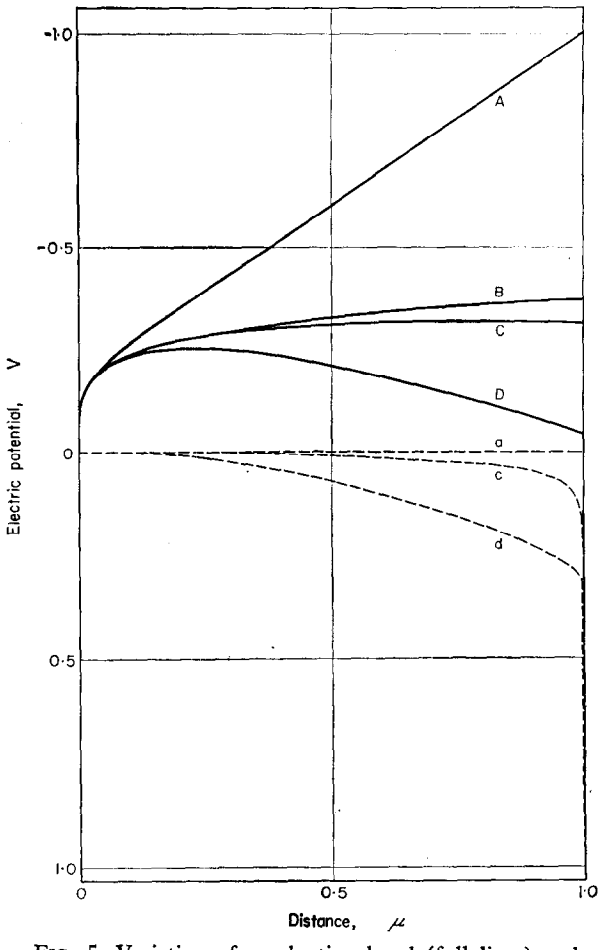

FIG. 5. Variation of conduction band (full lines) and Fermi-level (broken lines) through the crystal for the current-carrying case; crystal thickness 1 μ. Curves A, a: zero-current case; curve B: first transition point, $j = 4{\cdot}78$ giving $-J = 2{\cdot}46$ A/cm^2; curves C, c: second transition point, $j = 15{\cdot}3$ giving $-J = 9{\cdot}16$ A/cm^2; curves D, d: $j = 3\times10^2$ corresponding to $-J = 200$ A/cm^2.

absolute position of the Fermi-level except near to the anode where the electron density falls extremely rapidly. It is not until drift mechanisms become predominant in the large-current range that there is any appreciable movement of the absolute position of the Fermi-level over most of the crystal.

We have seen that for currents above the transition range carrier drift is the predominant mechanism; it is now appropriate to discuss this range in which current follows a very nearly square-law dependence on applied voltage.

(c) *Square-law current range.* We have seen that in this range the quantity α^2 is large and negative but $j \gg \alpha^2$ numerically. Accordingly, the situation must be described in terms of Bessel J functions in the cathode regions of the crystal and in terms of I functions in the anode regions. Since $j \gg \alpha^2$ we have z_1 large, and once again the asymptotic expansions of the I functions may be used in equation (27b) for β to obtain to the degree of accuracy required

$$-\beta = \frac{12z_1e^{z_1} + \cos\frac{\pi}{6}\cdot e^{-z_1}}{12z_1e^{z_1} - \cos\frac{\pi}{6}\cdot e^{-z_1}} \qquad (38)$$

In deriving this expression the negative sign for $\sqrt{(B_1)}$ has been used because $\mathscr{E}_1$ is now negative. This expression is valid provided

$$1/12z_1 \gg [\sqrt{(B_1)}-1]/2 \simeq bn_1/4jN_0$$

which is true in this current range. Since z_1 is large it is evident that $-\beta$ is again almost equal to unity; this time, however, $-\beta$ is slightly greater than unity. As before, the slight deviation of $-\beta$ from unity is significant in evaluating conditions in the anode regions of the crystal, since we are once again concerned with the very small difference between two very large quantities.

Considering now conditions near the cathode, we have, since $j \gg \alpha^2$, that $z \ll z_1$; thus it is sufficiently accurate to take $-\beta$ as equal to unity in the cathode regions of the crystal. Turning now to equation (23) for the electron density it is apparent that the quantity

$$[J_{-1/3}(z_0)+J_{1/3}(z_0)]$$

must be near zero, because B_0 is very large. Since B_0 is so large it is sufficiently accurate to take z_0 to be a zero of this quantity. Taking the first zero to avoid potential infinities in the crystal we find $z_0 = 2{\cdot}38(3)$ giving

$$-\alpha^2 = 2{\cdot}946j^{2/3} \qquad (39)$$

This result provides the value of α^2 in the square-law current range.

Returning to equation (21), the electric potential

in the crystal is given by

$$\exp(\mathscr{V}-\mathscr{V}_0)=\left(\frac{z_0}{z}\right)^{2/3}\left[\frac{J_{-1/3}(z_0)+J_{1/3}(z_0)}{\beta I_{-1/3}(z)+I_{1/3}(z)}\right]^2$$

In this expression the quantity

$$[J_{-1/3}(z_0)+J_{1/3}(z_0)]$$

is very small and it is preferable to substitute for it in terms of B_0 from equation (23) for the electron density. We then obtain

$$\exp(\mathscr{V}-\mathscr{V}_0)=\left(\frac{z_0}{z}\right)^{2/3}\frac{1}{B_0}\left[\frac{J_{-2/3}(z_0)+J_{2/3}(z_0)}{\beta I_{-1/3}(z)+I_{1/3}(z)}\right]^2 \tag{40}$$

In the vicinity of the cathode where $js<\alpha^2$ numerically, this result must be expressed entirely in terms of Bessel J functions. In the anode regions of the crystal z is sufficiently large that the asymptotic expansions of the I functions may be used. In order to obtain the current–voltage characteristics of the crystal we put $z=z_1$ to obtain

$$\exp(\mathscr{V}_a-\mathscr{V}_0)=\frac{2{\cdot}40\pi}{B_0}\left(\frac{z_0}{z_1}\right)^{2/3}z_1e^{2z_1} \tag{41}$$

In this result $\mathscr{V}_a-\mathscr{V}_0$ is, as before, the reduced inner potential across the crystal. It may be noted that this expression is now independent of n_1, the electron density at the anode contact. Thus, in this current range, physical conditions and current mechanisms in the crystal are independent of the precise nature of the anode contact provided that it is a blocking contact, for which the ratio n_1/N_0 is very small. However, it should be remembered that the magnitude of the external applied voltage which is required to produce a given current density does depend on the nature of the anode contact since the external voltage must include the work-function difference between anode and cathode metals.

Combining equations (39) and (41) we obtain

$$-J\left(1-\frac{3}{j^{1/3}}\right)^3=\frac{9\epsilon\mu}{8d^3}(V_a-V_0)^2\left(1+\frac{kT}{e(V_a-V_0)}\log D\right)^2 \tag{42}$$

where $D=B_0/2{\cdot}40\pi z_1^{1/3}z_0^{2/3}$

This shows that the current follows an approximately square-law dependence upon the applied inner potential difference. The external applied potential difference is given by $V_a'=V_a-V_1$ where $V_1=-\phi_1/e$. This expression is useful for the thicker crystals ($d>10\mu$) in which current of practical magnitude is not reached until drift mechanisms become effective; it provides an accurate description of current–voltage relations for large currents for which drift-current mechanisms are predominant. The range of validity of this result is determined by the requirements that $\sqrt{(B_0)}\gg 1$ and $(1+\beta)\simeq 0$; provided that $j>100$ these requirements are satisfied and equation (42) is accurate. Unfortunately this equation is tedious to use for the calculation of current–voltage characteristics because of the complicated nature of the quantity D. However a considerable simplification can be effected by neglecting the slight dependence of the logarithmic term upon temperature and applied voltage. In this way we obtain

$$-J\left(1-\frac{3}{j^{1/3}}\right)^3=\frac{9\epsilon\mu V_a^2}{8d^3}\left(1+\frac{pkT}{eV_a}\right)^2 \tag{43}$$

This expression is readily manipulated for the purposes of calculation. The reduced-current density j is given in terms of the physical parameters by equation (7). The quantity p is equal to

$$\log\left[d^2e^2N_0/7{\cdot}2\sqrt{(2)}\pi\epsilon kTj^{1/3}(j+\alpha^2)^{1/2}\right]$$

It varies only slowly with temperature and applied voltage and a value $p=11$ calculated for $T=300k$, $j=1000$, covers practical ranges of temperature and applied voltage. As j increases, the magnitude of B_0 falls and α^2 begins to deviate from the value given by equation (39). However, when the current density, and therefore the applied voltage, is large equation (42) reduces to

$$-J=\frac{9\epsilon\mu}{8d^3}(V_a'+V_1-V_0)^2 \tag{44}$$

and is independent of α^2. Except for the introduction of the work-function threshold $-(V_1-V_0)$ this is in fact the approximate result obtained by MOTT and GURNEY on the basis of a drift mechanism alone.

The physical meaning of this result is clear and can be discussed with reference to Fig. 3. In the

vicinity of the ohmic contact to the crystal a space-charge cloud of electrons forms. Current occurs when electrons are drawn from this space-charge reservoir by the applied voltage. Accordingly, electron emission into the crystal occurs from a "virtual cathode" within the crystal. The effective thickness of the crystal is thus reduced by a factor $(1-3/j^{1/3})$. At the virtual cathode the electric potential rises to a maximum (negative) value and then falls rapidly to the anode. Accordingly the effective voltage across the crystal is increased by a factor

$$[1+kT(\log D)/e(V_a-V_0)]$$

Both of these effects are caused by diffusion mechanisms and assist forward current.*

The variation of electric potential through the crystal is shown in Fig. 6 for various increasing values of current through the large-current range. These results have been obtained from equation (40) and show very well the existence of the virtual cathode and the way in which it gradually becomes eliminated as the current increases. These curves refer to a crystal 10 μ thick at a temperature of 300°K for which, as before, the electron mobility $\mu = 0{\cdot}10$ m^2/V-sec and the permittivity $\epsilon = 10^{-10}$ F/m.

The current–voltage characteristic of the crystal is shown in Fig. 7. The abscissa of this diagram gives the external applied voltage and the ordinate gives the square-root of the SCL current density. The diagram shows that there is a small voltage threshold before significant forward current is obtained. This threshold arises basically in the work-function difference $(\phi_1-\phi_0)$ between anode and cathode metals but is reduced to some extent by the effects of carrier diffusion in the crystal. Above this threshold current follows a very nearly square-law dependence upon applied voltage. This is, of course, the solid-state analogue of the three-halves law for SCL current in vacuum. Slight deviations from the exact square-law relation are caused by the contribution of carrier-diffusion mechanisms to the current. At larger currents, for thicker crystals, or at lower temperatures, carrier diffusion becomes less important and the exact square-law characteristic is more nearly approached.

The broken curve in this diagram gives the current–voltage characteristic for a crystal provided with a more highly blocking anode for which $-(\phi_1-\phi_0)/e$ is 2 eV. As expected, the only difference this makes is to shift the curve by 1 V to higher voltages.

The Fermi-level in the crystal may be found by using equation (23) to obtain the electron density in the crystal and then using the relation $n = N_0 \exp(-W_f/kT)$. The variation of Fermi-level is shown in Fig. 8 for the same values of current as used in Fig. 6. The interesting feature of these curves is that the Fermi-level increases rapidly on leaving the cathode then becomes almost constant but increasing slowly over the greater part of the crystal and finally rises extremely rapidly near the anode. This diagram illustrates that near the cathode the electron density falls rapidly from the very large value n_0 to a much lower value which does not vary much over the greater part of the crystal until the vicinity of the anode is reached where the electron density falls extremely rapidly to the very low value n_1. The increase in Fermi-level near the anode occurs extremely sharply over a distance much smaller than an electron mean free path and therefore does not have any physical significance. Because the Fermi-level is so nearly constant over most of the crystal it is justifiable to make a distinction between shallow trapping levels and deep trapping levels as discussed in Section 2; for all practical purposes electron traps at a depth W_t less than 0·3 eV below the conduction band may be regarded as shallow.

In the immediate vicinity of the cathode and anode contacts, current is carried predominantly by carrier diffusion even though carrier drift is the predominant mechanism over most of the crystal. Since physical conditions in the vicinity of the contacts are considerably different from those obtaining over the bulk of the crystal it is of interest to consider the contact regions in more detail.

In the vicinity of the cathode the electron space-charge density is high and the electron atmosphere is very little affected by the occurrence of current. Thus in the cathode region of the crystal, conditions deviate only slightly from the zero-current situation. This may be demonstrated with reference to the electric field at the cathode; for large currents we obtain from equation (35) that

$$\mathscr{E}_0 = (2bn_0/N_0+2\alpha^2)^{1/2} \qquad (45)$$

* This does not imply, of course, that the virtual cathode is at a distance $3d/j^{1/3}$ from the actual cathode or that the height of the potential maximum is $kT(\log D)/e$.

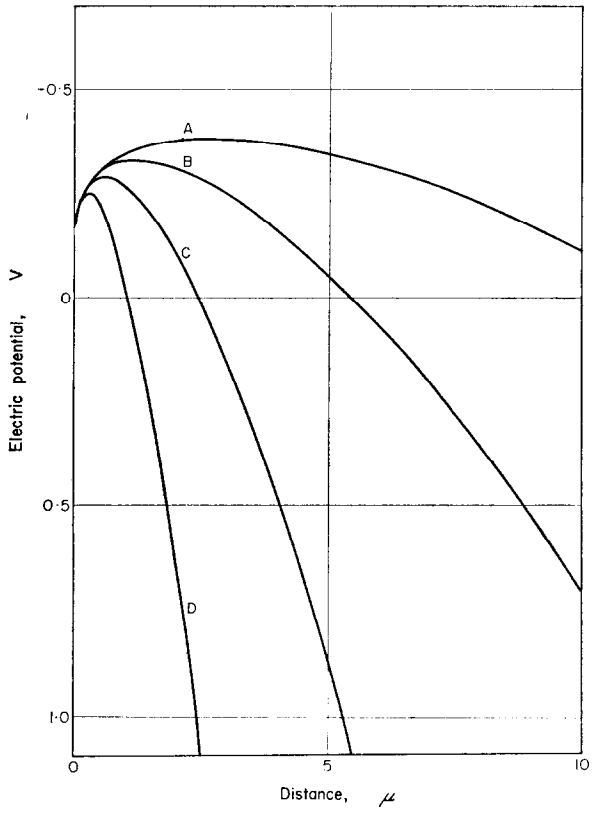

FIG. 6. Variation of conduction band through the crystal for large currents; crystal thickness 10 μ. Curve A: $-J = 0{\cdot}20$ A/cm^2; curve B: $-J = 2{\cdot}0$ A/cm^2; curve C: $-J = 20$ A/cm^2; curve D: $-J = 200$ A/cm^2.

Now in this current range $\alpha^2 \ll bn_0/N_0$; consequently this is very nearly the same as the zero-current result

$$\mathscr{E}_0 = (2bn_0/N_0 + 2g^2)^{1/2} \qquad (46)$$

The situation near the anode is more interesting. As the current increases the electron space-charge density spreads towards the anode; in the immediate vicinity of the anode, however, the electron density falls rapidly to the relatively very small value n_1. Since z is large near the anode we may use the asymptotic expansions of the Bessel I functions in equations (23) and (27b)* to obtain

* Equation (38) for β is not sufficiently accurate for this purpose; additional terms must be included from the expansion of the Bessel functions.

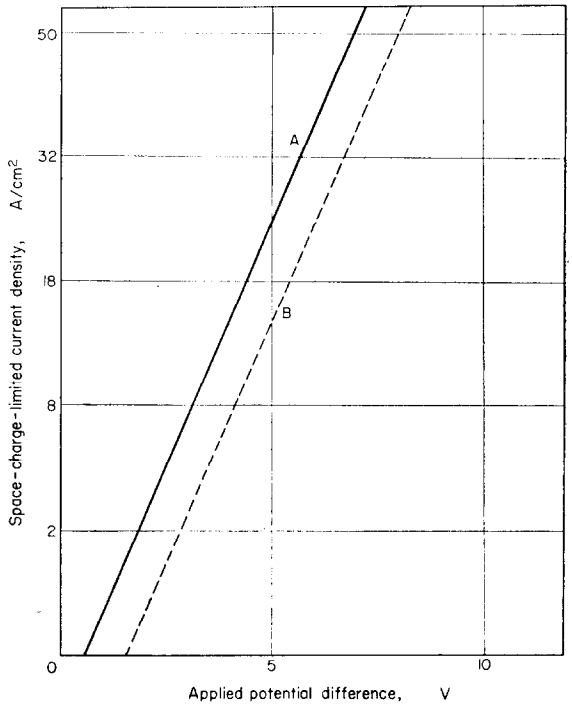

FIG. 7. Forward current–voltage characteristic of space-charge-limited current; crystal thickness 10 μ. Curve A: $(\phi_1 - \phi_0) = 1{\cdot}0$ eV; curve B: $(\phi_1 - \phi_0) = 2{\cdot}0$ eV.

$$\frac{n}{N_0} = \frac{js+\alpha^2}{b}\left(\frac{1}{3z} - \frac{\exp[2(z_1-z)]}{3z_1}\right) \qquad (47)$$

This expression provides an accurate description of the electron density in the anode regions of the crystal where z is large. At the anode contact itself, however, it gives the value $n_1/N_0 = 0$ instead of the true but very small value $n_1/N_0 = 10^{-16{\cdot}12}$. As we have already seen, however, the precise value of n_1 at the anode contact is immaterial in this current range.

As the current increases through the square-law current range, equation (39) shows that the quantity $-\alpha^2$ increases. The magnitude of B_0, therefore, gradually decreases and the value of z_0 required to satisfy equation (23) gradually decreases. This does not significantly affect the result given by equation (42) because at the larger currents the applied voltage is large. However, this variation of B_0 must be taken into account when discussing current mechanisms in the immediate vicinity of the cathode contact.

If the applied voltage is increased to very large values it will eventually become sufficiently large to move the whole cathode space-charge reservoir across the crystal and the current will saturate and become proportional to applied voltage.

(d) *Saturation-current range.* At very large applied voltages the electric-field intensity in the crystal will be very nearly uniform, and equal to $-V_a'/d$. Turning to equation (25) this can provide a suitable result only if α^2 is positive and very large and if the magnitude of the reduced field intensity is given by $-\sqrt{(2)}\alpha$. We thus have that

$$\mathscr{E} = -\mathscr{V}_a' = -\sqrt{(2)}\,\alpha \qquad (48)$$

in the saturation-current range. In particular, the electric-field intensity at the cathode has decreased from positive values in the large-current range, passed through zero, and is now going large and negative.

Now we have seen that, in the square-law current range, the quantity α^2 increases negative as the current increases. Referring again to equation (25) this shows that the field intensity at the cathode is decreasing and does in fact become zero when $\alpha^2 = bn_0/N_0$. If α^2 became larger than bn_0/N_0 the equation would imply an imaginary field intensity at the cathode. This is not physically permissible and we conclude therefore that the maximum negative value of α^2 is bn_0/N_0 which it reaches as $\mathscr{E}_0$ becomes zero. Subsequently α^2 decreases negative, passes through zero, and increases large and positive into the saturation-current range.

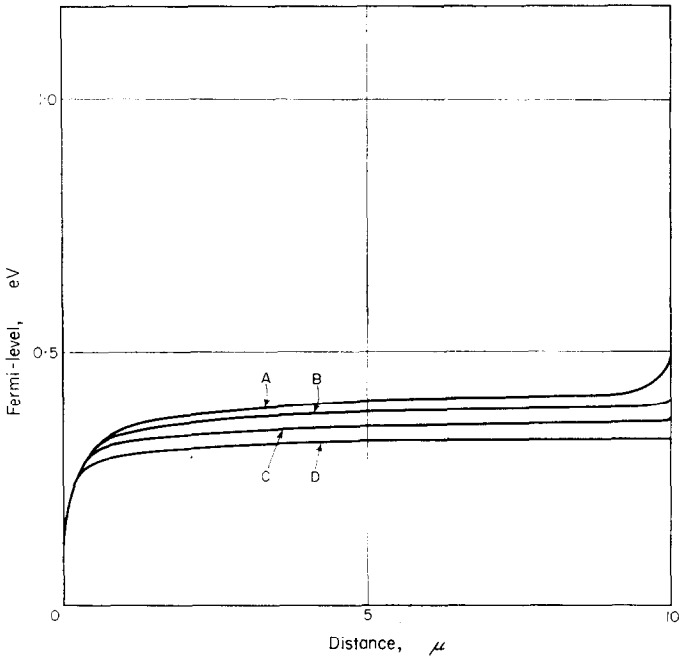

FIG. 8. Variation of Fermi-level through the crystal for currents in the square-law range; crystal thickness 10 μ. Curve A: $-J = 0{\cdot}20$ A/cm^2; curve B: $-J = 2{\cdot}0$ A/cm^2; curve C: $-J = 20$ A/cm^2; curve D: $-J = 200$ A/cm^2.

While the integration constant α^2 is varying in this way z_1 is increasing steadily and equation (38) shows that $-\beta$ remains very nearly equal to unity. Referring now to equation (23) we see, when $\alpha^2 = bn_0/N_0$ and B_0 is zero, that the quantity

$$[J_{2/3}(z_0)+J_{-2/3}(z_0)]$$

is zero. Accepting the first zero as before we have $z_0 = 0{\cdot}685$. This provides a fixed point between

the large-current and saturation-current ranges. Taking again the case of a crystal 10 μ thick at a temperature of 300°K with $\mu = 0{\cdot}1\ \mathrm{m^2/V\text{-}sec}$ and $\epsilon = 10^{-10}\ \mathrm{F/m}$, and using $eV_0 = 0{\cdot}1$ eV, we obtain, when the electric field at the cathode is zero, that $j = 4{\cdot}07\times10^9$ giving $-J = 2{\cdot}74\times10^6\ \mathrm{A/cm^2}$. Evidently when the crystal is provided with an ohmic cathode the saturation-current range is far above any practical current range; accordingly it will not be discussed further.

So far this discussion has been concerned with forward current; it is now appropriate to discuss the reverse-current case.

B. *Reverse-current case*

With a blocking anode, current in the reverse direction will always be very small. For small reverse voltage in particular, conditions near the cathode will not be significantly different from the zero-current case. Once again therefore we deduce that α^2 is not very different from g^2. At very large reverse voltage, however, the electric-field intensity in the crystal will be effectively uniform and very nearly equal to $-V_a'/d$. Turning to equation (25) for the field intensity this can only provide the correct result if α^2 is very large and positive and if the magnitude of the field intensity is given by $+\sqrt{(2)}\alpha$. At large reverse voltages, therefore, α^2 is very large and positive and we always have $j \ll \alpha^2$. It follows from this that z is everywhere large and real so that Bessel I functions may be used throughout.

Turning to equations (27a) and (27b) for β it is necessary to use the positive sign for $\sqrt{(B_0)}$ and $\sqrt{(B_1)}$ since the electric-field intensity is everywhere positive. However, since the quantities z_0 and z_1 are negative in the reverse-current case, we obtain the same result for β by using the negative sign for $\sqrt{(B)}$ and taking z positive. This case has been evaluated previously to provide equation (38); to the rather greater degree of accuracy required here we have

$$-\beta = \frac{[\sqrt{(B)}+1]e^z - \{\sqrt{(B)}-1-[7+5\sqrt{(B)}]/72z\}\,(\cos\pi/6)e^{-z}}{[\sqrt{(B)}+1]e^z + \{\sqrt{(B)}-1-[7+5\sqrt{(B)}]/72z\}\,(\cos\pi/6)e^{-z}} \qquad (49)$$

In this result of course the quantities $\sqrt{(B)}$ and z are to be regarded as positive because algebraic sign has been taken into account in the derivation.

Using cathode and anode conditions and equating the two expressions for β obtained from equation (49) we have:

$$\exp[2(z_1-z_0)] = [(B_1-1)/4-1/12z_1]\times \times[\sqrt{(B_0)}+1]/[\sqrt{(B_0)}-1] \qquad (50)$$

For the particular case of zero reverse current this expression reduces to the zero-current case discussed in Section 3.

Equations (49) and (50) may be used to provide the integration constants α^2 and β relevant to the reverse-current case. In particular the current–voltage characteristic of the crystal is obtained using equation (21) together with equation (50) to give

$$\exp(\mathscr{V}_a-\mathscr{V}_0) = \frac{B_1-1}{B_0-1} - \frac{1}{3z_1(B_0-1)} \qquad (51)$$

which reduces to

$$-J = \sqrt{(2)}\alpha\mu kTn_1[\exp(eV_a'/kT)-1]/d \qquad (52)$$

For very small reverse current, conditions in the crystal are not very different from zero-current conditions and we may write $\alpha^2 = g^2$. Thus we have the same result as for very small forward current except that the signs of current and applied voltage have reversed. This shows that the current–voltage characteristic has the same slope on either side of zero voltage.

When the reverse voltage is large ($eV_a' \gg kT$) equation (52) shows that $\sqrt{(2)}\alpha = jN_0/bn_1$. Combining equations (50) and (51) we obtain

$$4\exp[-\sqrt{(2)}\alpha] = [\sqrt{(B_0)}+1]^2\exp(\mathscr{V}_a-\mathscr{V}_0) \qquad (53)$$

This equation provides the value of α^2 for large reverse voltage. In particular, when

$$-(\mathscr{V}_a-\mathscr{V}_0) \gg (2bn_0/N_0)^{1/2}$$

we have

$$-\sqrt{(2)}\alpha = (\mathscr{V}_a-\mathscr{V}_0)$$

from which it follows that

$$J = n_1e\mu[-V_a'-(V_1-V_0)]/d \qquad (54)$$

In this expression V_a' is the reverse applied voltage and is negative, and V_1 and V_0 are each negative as usual. This result shows, as expected, that, at large reverse voltages, current is proportional to applied voltage. With a blocking anode, for which the ratio n_1/N_0 is very small, the reverse current is always very small.

6. REMARKS

The experimental achievement of SCL current in cadmium sulphide crystals has shown that the mechanism of defect compensation is very successful in eliminating the influence of empty, deep trapping levels. Possible practical applications for SCL current in the development of high-frequency, low-noise and temperature-insensitive solid-state devices have been discussed elsewhere[6,8,31–33] and it is of interest here to consider some possible applications in fundamental solid-state research.

ROSE[1], LAMPERT[9] and SMITH[34], in particular, have pointed out that in uncompensated crystals the voltage dependence and temperature dependence of SCL current are sensitive to extremely small densities of deep trapping defects. It has been suggested by them that this could be used to provide information about the density and energy distribution of trapping levels. An alternative approach for the investigation of trapping levels, particularly in compensated crystals in which large SCL current can be obtained, may be to study the temperature and frequency dependence of current fluctuations. In this connexion, the intrinsic level of fluctuations caused by variations in stored charge and by variations in transit time should be extremely small under SCL conditions. Accordingly if the trap density is sufficiently high the predominant mechanism of current fluctuations will be variations in the number of mobile carriers due to exchange of carriers between conduction and trapping levels. Further information about trap depths, densities and lifetimes may be obtained by studying the frequency dependence of current, particularly for the case of shallow traps.[31, 33] These methods for studying electron traps are complementary and could form the basis of a useful technique for studying some aspects of the defect solid state particularly in wide band-gap materials.

In compensated crystals the magnitude of current in the square-law range is a direct measure of carrier mobility and can be used to provide the magnitude of this quantity over a wide range of temperature and applied field strength. This is of interest because the density of such additional scattering centres as ionized donor centres can be brought to a minimum and the observed mobility be more truly representative of lattice scattering. In this connexion, the number of carriers available for current is not influenced much by temperature changes; consequently measurements can be made readily over wide temperature ranges. Furthermore, by using the thicker crystals ($d > 10\ \mu$), high electric fields can be applied without resulting in undue power dissipation in the crystal, and the investigation of field dependence of mobility facilitated.

The voltage threshold for forward current in the square-law current range provides a measure of the zero-current inner potential difference across the crystal. In the practical case, in which the cathode energy step is made as small as possible, this gives the magnitude of the anode energy step which for the ideal contact is equal to the difference between the work function of the anode metal and the electron affinity of the crystal. In principle, therefore, this can provide the absolute position of the electron-energy band system of the crystal, information which at present is virtually non-existent for wide band-gap materials and is necessary to complement theoretical studies of electron band structures and to aid understanding of surface and contact phenomena.

Electrical properties such as photoconductivity and breakdown are influenced partially and in some instances predominantly by contact effects. The measurement of forward SCL characteristics can provide information about defects in the crystal and about the magnitude of the anode energy step to assist the interpretation of measurements of photoconductivity, high field conduction, or electric breakdown subsequently made in the reverse direction and for which the anode contact would act as a normal contact.

7. CONCLUSIONS

This discussion of SCL current in solids has produced some clarification of the physics of the metal–insulator contact. Carrier-concentration gradients and space-charge inevitably exist in the vicinity of any contact, and this detailed discussion

of the simplest case, showing that current is carried predominantly by carrier diffusion near ohmic and blocking contacts, provides qualitative information about more complex cases as, for example, the metal–semiconductor contact and the metal–photoconductor contact.

The discussion has shown that a number of current ranges can be defined on the basis of the physical conditions existing in the crystal. Simple and accurate expressions have been obtained describing in particular current mechanisms and characteristics for small forward currents when diffusion mechanisms are predominant, and for large forward currents when drift mechanisms are predominant. The overall current–voltage characteristics are illustrated in Fig. 9 which shows the calculated characteristics of two crystals with thicknesses of 1 μ and 10 μ, respectively, and having permittivity 10^{-10} F/m and electron mobility 0·1 m^2/V-sec.

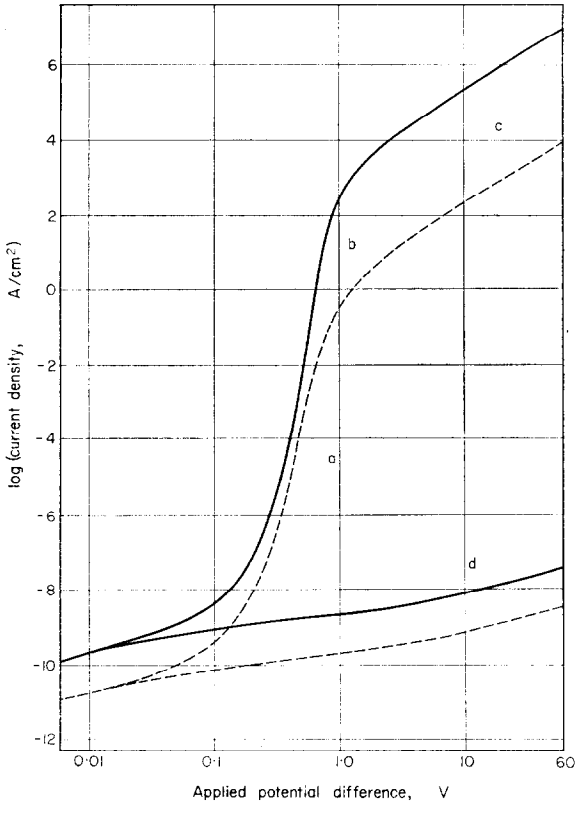

FIG. 9. Current–voltage characteristics of space-charge-limited current; crystal thickness 1 μ (full lines) and 10 μ (broken lines). Forward characteristic: (a) exponential range, (b) transition range, (c) square-law range. Reverse characteristic: (d).

At small forward voltage [region (a)] current occurs against the direction of the electric field in the crystal and takes place by the predominant mechanism of carrier diffusion. The current increases approximately exponentially with applied voltage and is very sensitive to temperature. For thin crystals and thin insulating layers ($d < 1\ \mu$), current of practical magnitude can be achieved in this current range.

With larger applied voltages [region (b)] the electric field reverses sign in the anode regions of the crystal and carrier drift now begins to assist carrier diffusion. This is the transition region in which the predominant current mechanism is changing from diffusion to drift and in which the virtual cathode begins to appear. The current increases steadily and smoothly with applied voltage although less rapidly than exponentially and there is no evidence for the existence of a negative-resistance region. The external applied voltage is still less than the work-function difference between anode and cathode metals.

When the applied voltage is of the order, or larger than, the work-function difference between anode and cathode metals [region (c)], the electric field over most of the crystal assists current, and carrier drift is the predominant mechanism of current. In this range, current is of practical magnitude and is very nearly proportional to the square of the applied voltage. Electron emission into the crystal takes place from a "virtual cathode" which exists in the cathode regions of the crystal. Since the effective density of carriers available for current is independent of temperature, current depends on temperature only through the variation of carrier mobility and the extent to which diffusion mechanisms contribute to current. Each of these effects is relatively small, and in any event they act in opposition; consequently in this range current is not very sensitive to temperature. The diagram illustrates well the sensitive dependence of current upon crystal thickness; in this square-law range current is proportional to the inverse cube of crystal thickness.

The Fermi-level in the crystal is nearly constant except near the cathode and near the anode. This

justifies the distinction made by ROSE between shallow traps which lie above the Fermi-level and deep traps which lie below it. This is significant because empty shallow traps merely reduce the magnitude of the current–voltage characteristics without affecting their form, whereas empty deep traps can reduce the magnitude and change the form of the current–voltage characteristics. Near the anode the Fermi-level rises extremely sharply as the electron density falls. However, most of this increase occurs over a distance which is much shorter than an electron mean free path and therefore cannot be used to describe the space-charge electron atmosphere in a real crystal. This means that in the practical case, and providing that the electron density at the anode contact is small compared with the electron density in the central regions of the crystal, the nature of the anode will affect only the magnitude of the forward voltage threshold and will not affect current mechanisms.

At very large forward voltage the whole of the space charge in the crystal is moved across the crystal, and saturation current is obtained proportional to the applied voltage. However, with an ohmic cathode this current range is far above any practical current range.

With a blocking anode for which the ratio n_1/N_0 is small, reverse current is small [region (d)]. As the applied voltage increases the zero-current space charge of electrons in the crystal is gradually swept out through the cathode contact and the resistance of the crystal increases; for large applied voltages it becomes constant and current is proportional to applied voltages. Since the electron space-charge density at the anode is very sensitive to temperature, the reverse current is very sensitive to temperature. Very high reverse resistance and consequently high rectification ratio can be achieved by using anode contacts of high work function.

The numerical calculations used to illustrate this discussion have been made on the basis of an electron mobility of 0·1 m^2/V-sec; this is intermediate between the value of 0·02 m^2/V-sec for cadmium sulphide and 0·9 m^2/V-sec for gallium arsenide. Although large and steady SCL current has so far been observed only in cadmium sulphide there seems no fundamental reason why it should not eventually be achieved in a wide range of materials. This would considerably increase the value of SCL current for basic research and for device development.

REFERENCES

1. A. ROSE, *Phys. Rev.* **97,** 1538 (1955).
2. R. W. SMITH, *Phys. Rev.* **97,** 1525 (1955).
3. G. F. ALFREY and I. COOKE, *Proc. Phys. Soc. Lond.* **70B,** 1096 (1957).
4. W. RUPPEL, *Helv. phys. acta* **31,** 311 (1958).
5. G. T. WRIGHT, *Nature, Lond.* **182,** 1296 (1958).
6. G. T. WRIGHT, *Proc. Instn. Elect. Engrs.* **B106,** 915 (1959).
7. A. CONNING, A. A. KAYALI and G. T. WRIGHT, *J. Instn. Elect. Engrs.* **5,** 595 (1960).
8. G. T. WRIGHT, *Electronics* **33,** 59 (1960).
9. M. A. LAMPERT, *Phys. Rev.* **103,** 1648 (1956).
10. R. L. LONGINI and R. F. GREENE, *Phys. Rev.* **102,** 992 (1956).
11. A. A. KAYALI, Thesis, University of Birmingham (1960).
12. J. W. ALLEN, *Nature, Lond.* **187,** 403 (1960).
13. G. C. DACEY, *Phys. Rev.* **90,** 759 (1953).
14. M. A. LAMPERT, *J. Appl. Phys.* **29,** 1082 (1958).
15. M. VON LAUE, *Jb. Radioakt.* **15,** 205, 257, 301 (1928).
16. R. H. FOWLER, *Statistical Mechanics.* Cambridge University Press (1936).
17. S. M. SKINNER, R. L. SAVAGE and J. E. RUTZLER, *J. Appl. Phys.* **24,** 438 (1953).
18. S. M. SKINNER, R. L. SAVAGE and J. E. RUTZLER, *J. Appl. Phys.* **25,** 1055 (1954).
19. D. C. WEST, *J. Appl. Phys.* **25,** 1054 (1954).
20. M. J. MORANT, *J. Appl. Phys.* **25,** 1053 (1954).
21. S. M. SKINNER, *J. Appl. Phys.* **26,** 498 (1955).
22. N. W. MCLACHLAN, *Ordinary Non-linear Differential Equations.* Clarendon Press, Oxford (1950).
23. N. F. MOTT and R. W. GURNEY, *Electronic Processes in Ionic Crystals.* Clarendon Press, Oxford (1940).
24. W. SHOCKLEY, *U.S. Pat.* 6978 (1953).
25. W. SHOCKLEY and R. C. PRIM, *Phys. Rev.* **90,** 753 (1953).
26. S. M. SKINNER, *J. Appl. Phys.* **26,** 509 (1955).
27. G. H. SUITS, *J. Appl. Phys.* **28,** 454 (1957).
28. W. SHOCKLEY, *Phys. Rev.* **56,** 317 (1939).
29. J. BARDEEN, *Phys. Rev.* **71,** 717 (1947).
30. F. A. KROGER, G. DIEMER and H. A. KLASENS, *Phys. Rev.* **103,** 279 (1956).
31. G. T. WRIGHT, *J. Brit. Instn. Radio Engrs.* **20,** 337 (1960).
32. G. T. WRIGHT, *New Scientist* **8,** 1704 (1960).
33. G. T. WRIGHT, *Digest, Solid State Circuits Conference, Philadelphia,* 1961.
34. R. W. SMITH, *R.C.A. Review* **20,** 69 (1959).